ASTANK2: Analytical Modeling and Simulation

Janetta CULIȚĂ, Dan ȘTEFĂNOIU, Alexandru DUMITRAȘCU
Faculty of Automatic Control and Computer Science
„Politehnica" University of Bucharest,
Bucharest, ROMANIA
E-mails: {janetta.culita, dan.stefanoiu, alexandru.dumitrascu}@acse.pub.ro

***Abstract*—The paper focuses on building the mathematical model of a filling/drainage process (namely ASTANK2), by analytical approach. Models are subsequently tested by simulation. The process is versatile: it consists of two tanks with different geometric shape, which could be considered in independent or coupled setup and are supplied by an adjustable water distribution pipelines network. The proposed model is nonlinear and can be defined in various configurations, by connecting the desired component models, from the available ones. A simulator that integrates these components is implemented in MATLAB-SIMULINK environment. Its goal is twofold: to simulate the plant dynamics according to several scenarios, on one hand, and to validate the proposed analytical model, on the other hand. Some simulation results are presented in the end.**

Keywords—water tanks, analytical modeling, nonlinear model, simulation.

I. INTRODUCTION

The fluid handling systems are essentially required in the vital process industries like energy, petro-chemical, water treatment or agriculture. Most of them rely on interactive multi-tanks, where the control of liquid level and flow between tanks represents a major and challenging concern, especially for they could be described as multi-variable systems with non-linear dynamics. Therefore, recently, the multi-tank processes have been capturing the interest of control engineering community. Hence, various control strategies, particularly the Model Predictive Control (MPC) techniques, have been designed and implemented on a four rectangular tanks system, as in [9] and [3].

Generally, the multi-tank processes addressed in the literature consist of two, three or four tanks, with cylindrical or rectangular shapes, which are interconnected in series or parallel configurations. For example, [7] mainly describes and analyses the model of the quadruple rectangular tank system. In [8], the nonlinear model of a three serially interconnected cylindrical tanks is presented in a multiple model approach (in view of state estimation). The process presented in [10] consists of three cylindrical tanks communicating by a sink and is modeled as an autonomous hybrid system. Besides the classical shape of tanks, there have been studied the conical and spherical tanks (like in [4] or [5]), whose irregular shapes introduce a supplementary nonlinearity in the analytical model. An interesting laboratory (didactical) installation belongs to INTECO Ltd. [2], which includes three interconnected tanks in cascade, two of them having irregular geometric shapes (one with a sloped wall and another one with a curved wall). The nonlinear analytical models presented in all above cited references derive from the volume conservation and fluid dynamics laws, which are applied at a macroscopic level of the liquid.

In this paper, the laboratory installation ASTANK2 (manufactured by ASTI Automation SRL [1]) is introduced, on modeling and simulation purpose. It was designed and implemented for education and research in modeling, identification and control, by using industrial instrumentation. As its name suggests, ASTANK2 is a two-tank coupled system, whose main feature is a sloped wall tank. This component adds a quadratic nonlinearity in the analytical model of the process, as shown in Section 3. The novelty of the paper consists in developing the model by considering the behavior of the fluid at the microscopic level. More specifically, one takes into account the gravity of one water molecule (which is decomposed along the sloped wall) and the number of the molecule comprised in the water volume, in order to compute the pressure developed by the liquid on the tank bottom. This approach is particularly valuable for sloped wall tanks modeling.

The outline of this paper is as follows. The next section is dedicated to a short general description of the plant ASTANK2. The analytical models of each component are introduced in section 3. The simulator integrating the models is described in section 4. Some simulation results obtained from different configuration scenarios are shown and discussed in section 5. The concluding remarks and a references list complete the article.

II. PLANT DESCRIPTION

The plant ASTANK2 represents a hydraulic system that includes two open tanks at the same height, as illustrated in Figure 1. The tanks are supplied with water from a third (accumulator) tank, by means of a pumping and distribution network. They can either be coupled through a baseline pipe or operate independently, depending on the "open/closed" position of the manually acted tap R. The drainage of the tanks is affected by the opening/closing of the taps R11 and R21. Thus, the process is versatile and the tank connectivity setup renders a wide range of experiments to develop.

Concerning the geometry of the upper tanks, there is a major difference between them. The first tank, on the left side, has a variable section, due to a sloped wall that introduces nonlinearity in its model, as outlined in the next section. The second tank, on the right side, is just a regular parallelepiped.

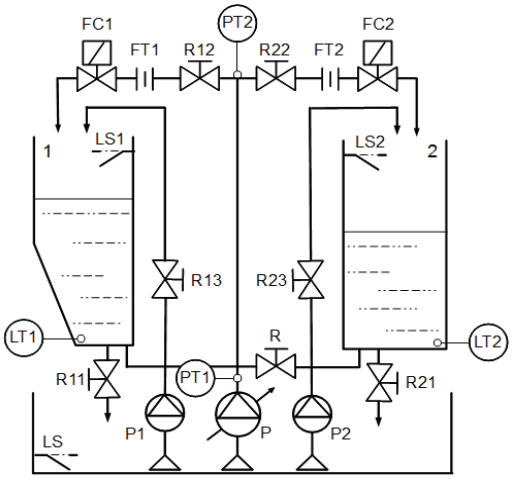

Fig. 1. ASTANK2 system

The water level in each upper tank is measured by using the level transducers LT1 and LT2 respectively. The level sensors LS1 and LS2 send overflow signals (if necessary), while the level sensor LS watches the low limit of the water level in the accumulator tank, in order to prevent the main pump P from dry functioning.

The main pump P (of March May MMP-2 type) is inverter-driven (SIEMENS, Sinamics G110, 0.25kW) and has the role to distribute the water from the accumulator tank in the system along the middle (main) vertical pipe. Its water flow and pressure can adaptively be set, by controlling the supplying frequency. The vertical pipe is branched at the upper side. The fluid pressure at the delivery and branching point is monitored by the pressure transducers PT1 and PT2 (SIEMENS, Sitrans P210). The latter sensor can send emergency signals on insufficient water quantity to fill up the branches simultaneously. On the horizontal tubes, two flow transducers, namely FT1 and FT2 (KOBOLD, DPL-1P20), are measuring the input flows in the tanks, which are controlled by the flow control electro-valves FC1 and FC2 (of Burkert 6024 type). The latter allows varying the flow rate by adjusting their voltage.

The main pumping system is completed by two auxiliary pumps P1 and P2 (EHEIM 1046), which allow adding a supplementary volume of liquid to each tank through the secondary vertical pipes. The auxiliary pumps ensure a constant flow in the pipes (by ON/OFF command) and were added in order to introduce disturbances in the filling/drainage process. The manual taps R13 and R23 could modify the perturbation flow rate in the pipes.

One can conclude that the water levels in the three tanks represent the measured parameters of the system, which depend on the following five input (control) parameters: the voltage applied to each electro-valve, the voltage applied on the main pump and the ON/OFF setting of the secondary pumps.

III. Analytical Modeling of ASTANK2

From the modeling point of view, ASTANK2 can be expressed by a multi-variable system with several linear/nonlinear blocks, as displayed in Figure 2.

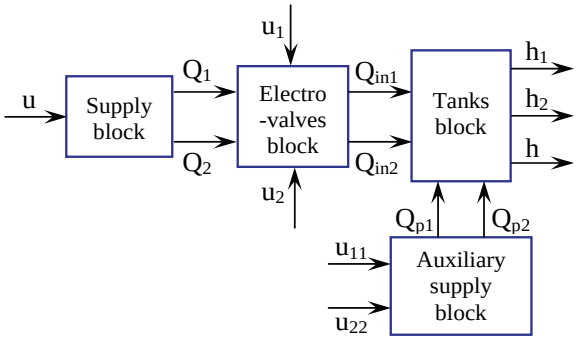

Fig. 2. ASTANK2 functional blocks and signals

The *supply block* includes the main pumping system and the flow transducers. It receives the control signal u (the voltage of the pump) and sends the signals Q_1 (the water flow in left branch) and Q_2 (the water flow in the right branch) to the electro-valve block. One assumes that a minimum volume of water is always available in the lower tank, such that the pump always pushes enough water to FCs. The feeding flow of the main pump is an internal variable and therefore not figured here. The *auxiliary supply block* includes the secondary pumping system. It receives the input control signals u_{11} and u_{22} (standing for the ON/OFF commands sent to the pumps) and sends to the tank block the output signals Q_{p1} and Q_{p2}. They are supplementary input flows in the upper tanks and play the role of perturbations that affect the filling/drainage process. The feeding flows of the secondary pumps also are considered as internal variables. The output signals simply result from the product between the input and the internal variables, which leads to a nonlinear model. The *electro-valves block* contains FC1 and FC2, which are in charge with adjusting the input flows of the upper tanks. Its input signals are: Q_1, Q_2 and the control signals u_1 and u_2 (the voltage supplied on FC1 and FC2, which are proportional to the percentages of valve aperture). The output signals are Q_{in1} and Q_{in2} (the effective supplying water flows for the upper tanks). The most complex block is the *tank block*, which comprises all the tanks in the plant. It describes the dependencies of the output signals h_1 (the current water level in the left side tank), h_2 (the current water level in the right side tank) and h (the current water level in the accumulator tank) on the input signals Q_{in1}, Q_{in2}, Q_{p1} and Q_{p2}. Although Q_{p1} and Q_{p2} play the role of disturbances in the process, for modeling and simulation purpose, they are considered as input signals, as well.

The analytical models of supply block, electro-valve block and tank block are described next, by taking into account their aforementioned input and output signals.

A. Supply block

The analytical model assigned to the supply block relies on the transfer functions of the pressure and flow transducers, as well as on the mathematical model of the flow process through the short upper pipe (between the branching point and the FC electro-valve). Both transducers are assumed to have linear characteristics. The gain of pressure transducer is $K_P = 1$. The flow transducer gain is $K_Q = 7.63$, while its time delay is $T_Q = 1\,\text{s}$. Thus, the transfer function of the flow sensor is: $H_Q(s) = 7.63 \cdot e^{-s}$.

The analytical model of the flow process through a short pipe is described by the equation below [6]:

$$\rho L_p \frac{dQ_{\{1,2\}}(t)}{dt} + \frac{\rho Q_{\{1,2\}}^2(t)}{2\alpha^2 S} = S\Delta P(t), \qquad (1)$$

where ΔP is the input signal (the differential pressure on the pipe), $Q_{\{1,2\}}$ are the output signals (the water flows in the left side and right side pipes, respectively, see Figure 2 again), ρ is the water density, S denotes the pipe section area, L_p is the pipe length and α stands for the discharge coefficient. The model of the supply block results by equating (1) for each horizontal pipe. The constructive parameters of the pipes are: $L_p = 0.04\,\text{m}$, $S = 0.00007854\,\text{m}^2$, $\alpha = 0.127$ (which is experimentally obtained from stationary flow regime).

B. Electro-valves block

A general nonlinear model of the electro-valve seemingly is the following:

$$T_{EV} \cdot \frac{dQ_{out}(t)}{dt} + Q_{out}(t) = \gamma(u_{EV}) \cdot Q_{in}(t), \qquad (2)$$

where Q_{in} denotes the input flow, Q_{out} represents the output flow, $\gamma(u_{EV})$ is the flow ratio, nonlinearly depending on the supplying voltage u_{EV}, whilst T_{EV} is the time delay of the electro-valve (whose value is known from the electro-valve characteristics). By adapting (2) to each electro-valve in the corresponding block and by employing the notations in Figure 2, the analytical model results in:

$$T_{EV} \cdot \frac{dQ_{\{in1,in2\}}(t)}{dt} + Q_{\{in1,in2\}}(t) = u_{\{1,2\}}(t) \cdot Q_{\{1,2\}}(t), \qquad (3)$$

where the time delay for the FC Burkert model is $T_{EV} = 0.0125\,\text{s}$.

C. Tanks block

The tanks block includes the upper tanks (that can be interconnected through the bottom pipe) and the accumulator tank. The analytical model of this block is expressed by equations including the output signals h_1, h_2, h and the input signals Q_{in1}, Q_{in2}, Q_{p1}, Q_{p2}. First, the component model of each individual tank is derived. Then, the global model is designed from the component models.

1) The left tank

The model of the left side tank is based on the schemata drawn in Figure 3(a), where the constructive parameters are specified as well.

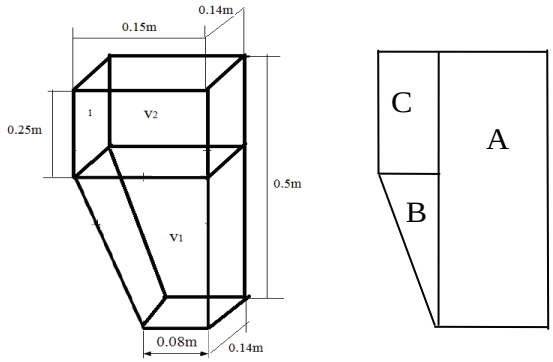

Fig. 3. The left side tank: (a) 3D view; (b) vertical section

One assumes that this tank is working independently on the right side tank. The analytical model is derived from the volume conservation equation:

$$\frac{dV_1(t)}{dt} = Q_{in1}(t) - Q_{out1}(t), \qquad (4)$$

where V_1 is the water volume corresponding to level h_1, whilst Q_{in1} and Q_{out1} stand for the volumetric charge and discharge flow of the tank, respectively.

The expression of the output volumetric flow Q_{out1} is developed by considering that the pressure force developed by the water on the tank bottom depends on the tank geometry and, consequently, on the current water volume. In this respect, the water volume is split into three components, as depicted in Figure 3(b): the parallelepiped A, the prism B and the parallelepiped C, each of which contributing independently to the pressure development.

Denote by L the length of the tank bottom, by l the tank width, by H the height of the sloped facet of the tank and by θ the sloping angle with respect to the vertical axis. Then, the water volume in each component, for a certain water level h_1 can be computed. Thus, the water volume in the parallelepiped A is $V_A = L \cdot l \cdot h_1$. The water volume in the prism B at a level $h_1 \le H$ is $V_B = \frac{l \cdot h_1^2 \cdot \tan\theta}{2}$. The water volume in the parallelepiped C can only be computed when $h_1 > H$. In this case, $V_C = l \cdot (h_1 - H) \cdot H \cdot \tan\theta$.

In order to evaluate the pressure force, one starts from accounting the gravity of a single water molecule, i.e. $F = m \cdot g$, where m is the molecule mass. As an important remark, only this type of force is considered here, since the

internal van der Waals attraction forces between molecules and between molecules and tank walls are too small and have been neglected. The same hypothesis is applied when expressing the contribution of the molecules gravity in each particular element of the tank, in order to compute the hydrostatic pressure.

Firstly, one computes the number of the molecules in the parallelepiped A:

$$N_m^A = \frac{V_A}{V_m} = \frac{L \cdot l \cdot h_1}{V_m}, \tag{5}$$

where V_m is the volume of one water molecule. Secondly, the pressure force developed by all N_m^A molecules on the tank bottom is equivalent to their total gravity and results in:

$$F^A = N_m^A \cdot F = m \cdot g \cdot \frac{L \cdot l \cdot h_1}{V_m}. \tag{6}$$

Consequently, the corresponding hydrostatic pressure P^A on the tank bottom is:

$$P^A = \frac{F^A}{L \cdot l} = \frac{m \cdot g \cdot h_1}{V_m} = \rho \cdot g \cdot h_1, \tag{7}$$

where ρ denotes the water density and $m = \rho V_m$.

In the prism B, the gravity of one liquid molecule is decomposed in two components. On one hand, there is the force $F_1 = m \cdot g \cdot \sin\theta$ that acts perpendicularly on the sloped wall and does not influence the pressure on the tank bottom, because of the sloped wall opposition. On the other hand, the force $F_2 = m \cdot g \cdot \cos\theta$ is parallel to the sloped wall and pushes the molecules in the A component. Moreover, the force F_2 is decomposed in two components as well. The force $F_{21} = m \cdot g \cdot \cos^2\theta$ acts perpendicularly on the tank bottom surface, while the force $F_{22} = m \cdot g \cdot \sin\theta \cdot \cos\theta$ is annihilated by the vertical wall of the tank.

The total number of molecules included into the B component is:

$$N_m^B = \frac{V_B}{V_m} = \frac{l \cdot h_1^2 \cdot \tan\theta}{2 \cdot V_m}, \tag{8}$$

while the global force transmitted by all N_m^B molecules on the tank bottom is :

$$F^B = mg \frac{l \cdot h_1^2 \cdot \tan\theta}{2V_m} \cdot \cos^2\theta = mg \frac{l \cdot h_1^2}{4V_m} \sin(2\theta). \tag{9}$$

Accordingly, the hydrostatic pressure P^B of the B component at the tank bottom is:

$$P^B = \frac{F^B}{L \cdot l} = mg \frac{h_1^2}{4V_m L} \sin(2\theta) = \rho g \frac{h_1^2}{4L} \sin(2\theta). \tag{10}$$

As of the parallelepiped C, the number of molecules is expressed by:

$$N_m^C = \frac{V_C}{V_m} = \frac{l\left(h_1 - H\right) \cdot H \cdot \tan\theta}{V_m}. \tag{11}$$

One can notice that the gravity transmitted by one molecule from the C body to the bottom surface of the A body is just F_{21} (as defined above), due to the same decomposition principle described for the B component. Then, the force transmitted by all molecules of the C parallelepiped to the bottom surface of the tank is:

$$\begin{aligned} F^C &= mg \frac{l \cdot \left(h_1 - H\right) \cdot H \cdot \tan\theta}{V_m} \cos^2\theta = \\ &= mg \frac{l \cdot \left(h_1 - H\right) \cdot H}{2V_m} \sin(2\theta). \end{aligned} \tag{12}$$

Thus, the hydrostatic pressure P^C of the C component at the tank bottom is:

$$P^C = \frac{F^C}{L \cdot l} = \rho g \frac{\left(h_1 - H\right)H}{2L} \sin(2\theta). \tag{13}$$

In conclusion, the expression of the global hydrostatic pressure P on the bottom of the left side tank is:

$$P(h_1) = \begin{cases} \rho g h_1 \left[1 + \frac{h_1}{4L} \sin(2\theta)\right] & , h_1 \le H \\ \rho g h_1 \left[1 + \frac{H}{2L} \sin(2\theta)\right] - \rho g \frac{H^2}{4L} \sin(2\theta) & , h_1 > H \end{cases}. \tag{14}$$

Note that, in the first case, the pressure parameter nonlinearly depends (by a quadratic variation) on the level h_1, while, in the second case, this variations is linear.

If S_1 is the section of the drainage pipeline, then Q_{out1} is expressed from the continuity equation $Q_{out1} = \alpha_1 S_1 v_1$, where v_1 represents the flow speed, whereas α_1 is a flow coefficient. The Bernoulli's law allows determining the flow speed: $v_1 = \sqrt{\frac{2\Delta P_1}{\rho}}$, where ΔP_1 is the differential pressure. Since the expression $a_1 = \alpha_1 S_1$ stands for a drainage specific constant of the tap R11 outlet (experimentally obtained), one can derive now Q_{out1} from equation (14):

$$Q_{out1} = \begin{cases} a_1 \cdot \sqrt{2\left[g h_1 \left[1 + \frac{h_1}{4L} \sin(2\theta)\right]\right]} & , h_1 \le H \\ a_1 \sqrt{2g h_1 \left[1 + \frac{H}{2L} \sin(2\theta)\right] - g \frac{H^2}{2L} \sin(2\theta)} & , h_1 > H \end{cases}. \tag{15}$$

The water volume V_1 in (4) is expressed as below, according to the values of h_1 in (14):

$$V_1(h_1)=\begin{cases} L\cdot l\cdot h_1+\dfrac{h_1^2\cdot l\cdot\tan\theta}{2} & ,h_1\le H \\ h_1\cdot l\cdot\left(L+H\cdot\tan\theta\right)-\dfrac{H^2\cdot l\cdot\tan\theta}{2} & ,h_1>H \end{cases}. \quad (16)$$

Thus, the analytical model (4) becomes:

a. if $h_1\le H$:

$$\left[L\cdot l+l\cdot\tan\theta\cdot h_1(t)\right]\frac{dh_1(t)}{dt}=Q_{in1}(t)- \\ -a_1\sqrt{2\left[gh_1(t)\left[1+\frac{h_1(t)}{4L}\sin(2\theta)\right]\right]}; \quad (17)$$

b. otherwise:

$$l\cdot\left(L+H\cdot\tan\theta\right)\cdot\frac{dh_1(t)}{dt}=Q_{in1}(t)- \\ -a_1\sqrt{2gh_1(t)\left[1+\frac{H}{2L}\sin(2\theta)\right]-g\frac{H^2}{2L}\sin(2\theta)}. \quad (18)$$

2) The right side tank

The second tank has the same constructive parameters as the A parallelepiped of the first tank (see Figure 3(b)), which leads to a simplified analytical model. As in equation (4), one starts from the volume conservation law:

$$\frac{dV_2(t)}{dt}=Q_{in2}(t)-Q_{out2}(t), \quad (19)$$

where V_2 is the water volume corresponding to level h_2, whilst Q_{in2} and Q_{out2} stand for the volumetric charge and discharge flow of the tank, respectively. Following a similar rationale as previously to compute the hydrostatic pressure at the tank bottom and exploiting again the Bernoulli's law, one obtains:

$$Q_{out2}=a_2\sqrt{2gh_2}, \quad (20)$$

where a_2 is a drainage constant associated to the outflow of the tank (through the tap R21). If A_2 is the cross-section area of the tank, the analytical equation of filling/drainage process results from equations (19) and (20):

$$A_2\frac{dh_2(t)}{dt}=Q_{in2}(t)-a_2\sqrt{2gh_2(t)}. \quad (21)$$

3) The accumulator tank model

As shown in Figure 1, the accumulator tank is filled with the discharged water from the upper tanks. Simultaneously, the water is pumped up through the main vertical pipe with a variable flow $Q(t)$, which is set by the pump P. The volume conservation law for the tank is then expressed as follows:

$$\frac{dV(t)}{dt}=Q_{out1}(t)+Q_{out2}(t)-Q(t), \quad (22)$$

where V is the water volume for a certain level h and the flow Q is an internal variable. Given the section area of the tank A_T, the analytical model derives from equations (15), (20) and (22):

a. if $h_1\le H$:

$$A_T\frac{dh(t)}{dt}=a_1\sqrt{2\left[gh_1(t)\left[1+\frac{h_1(t)}{4L}\sin(2\theta)\right]\right]}+ \\ +a_2\sqrt{2gh_2(t)}-Q(t); \quad (23)$$

b. otherwise:

$$A_T\frac{dh(t)}{dt}=a_1\sqrt{2gh_1(t)\left[1+\frac{H}{2L}\sin(2\theta)\right]-g\frac{H^2}{2L}\sin(2\theta)}+ \\ +a_2\sqrt{2gh_2(t)}-Q(t). \quad (24)$$

4) The overall tank model

The upper tanks could be interconnected in series configuration by keeping the coupling tap R open (see Figure 1 again). The well-known nonlinear expression of the communicating flow Q_c, available from physics (presented in [7]), is derived here by employing the pressure model (14), instead of ρgh_1:

$$Q_c=a_c\,\mathrm{sign}\left(P(h_1)-\rho gh_2\right)\sqrt{\frac{2\left(P(h_1)-\rho gh_2\right)}{\rho}}, \quad (25)$$

where a_c is the drainage constant associated to tap R and the sign function highlights the flow direction in this pipe.

Consider now the general configuration of the process. Thus, besides the current flows Q_{in1} and Q_{in2}, the upper tanks can be supplied by means of the supplementary flows Q_{p1} and Q_{p2}, which are pumped up in the system from the accumulator tank through the secondary pumps. In this context, the equations (4), (19) and (22) lead to the system of analytical equations below:

$$\begin{cases} \dfrac{dV_1(t)}{dt}=Q_{in1}(t)+Q_{p1}(t)-Q_{out1}(t)-Q_c(t) \\ \dfrac{dV_2(t)}{dt}=Q_{in2}(t)+Q_{p2}(t)-Q_{out2}(t)+Q_c(t) \\ \dfrac{dV(t)}{dt}=Q_{out1}(t)+Q_{out2}(t)-Q(t)-Q_{p1}(t)-Q_{p2}(t) \end{cases}. \quad (26)$$

The model (26) can furthermore be detailed. Focus first on the case $h_1\le H$. Then, by using the equations (14), (17), (21) and (23) in the system (26), the generic tank model becomes:

$$\left[L\cdot l+l\cdot h_1(t)\cdot\tan\theta\right]\frac{dh_1(t)}{dt}=Q_{in1}(t)+Q_{p1}(t)-$$
$$-a_1\sqrt{2\left[gh_1(t)\left[1+\frac{h_1(t)}{4\cdot L}\sin(2\theta)\right]\right]}-$$
$$-a_c\,\mathrm{sign}\left(h_1(t)-h_2(t)+\frac{h_1^2(t)}{4L}\sin(2\theta)\right)\times$$
$$\times\sqrt{2g\left[h_1(t)-h_2(t)+\frac{h_1^2(t)}{4L}\sin(2\theta)\right]}; \quad (27)$$

$$A_2\frac{dh_2(t)}{dt}=Q_{in2}(t)+Q_{p2}(t)-a_2\cdot\sqrt{2gh_2(t)}+$$
$$+a_c\,\mathrm{sign}\left(h_1(t)-h_2(t)+\frac{h_1^2(t)}{4L}\sin(2\theta)\right)\times$$
$$\times\sqrt{2g\left[h_1(t)-h_2(t)+\frac{h_1^2(t)}{4L}\sin(2\theta)\right]}; \quad (28)$$

$$A_T\frac{dh(t)}{dt}=a_1\sqrt{2\left[gh_1(t)\left[1+\frac{h_1(t)}{4L}\sin(2\theta)\right]\right]}+$$
$$+a_2\sqrt{2gh_2(t)}-Q(t)-Q_{p1}(t)-Q_{p2}(t). \quad (29)$$

In the second case, $h_1>H$, the corresponding equations (14), (18), (21) and (24) are inserted into the system (26), in order to derive the generic tank model. It follows:

$$l\left(L+H\cdot\tan\theta\right)\frac{dh_1(t)}{dt}=Q_{in1}(t)+Q_{p1}(t)-$$
$$-a_1\sqrt{2gh_1(t)\left[1+\frac{H}{2L}\sin(2\theta)\right]-g\frac{H^2}{2L}\sin(2\theta)}-$$
$$-a_c\,\mathrm{sign}\left(h_1(t)-h_2(t)+\frac{h_1(t)H}{2L}\sin(2\theta)-\frac{H^2}{4L}\sin(2\theta)\right)\times$$
$$\times\sqrt{2g\left[h_1(t)-h_2(t)+\frac{h_1(t)H}{2L}\sin(2\theta)-\frac{H^2}{4L}\sin(2\theta)\right]}; \quad (30)$$

$$A_2\frac{dh_2(t)}{dt}=Q_{in2}(t)+Q_{p2}(t)-a_2\sqrt{2gh_2(t)}+$$
$$+a_c\,\mathrm{sign}\left(h_1(t)-h_2(t)+\frac{h_1(t)H}{2L}\sin(2\theta)-\frac{H^2}{4L}\sin(2\theta)\right)\times$$
$$\times\sqrt{2g\left[h_1(t)-h_2(t)+\frac{h_1(t)H}{2L}\sin(2\theta)-\frac{H^2}{4L}\sin(2\theta)\right]}; \quad (31)$$

$$A_T\frac{dh(t)}{dt}=a_1\sqrt{2gh_1(t)\left[1+\frac{H}{2L}\sin(2\theta)\right]-g\frac{H^2}{2L}\sin(2\theta)}+$$
$$+a_2\sqrt{2gh_2(t)}-Q(t)-Q_{p1}(t)-Q_{p2}(t). \quad (32)$$

In order to complete the modeling, the constructive parameters of ASTANK2 and the flow coefficients have to be specified. Some of them have already been referred inside this section. The others are: $\theta=15^\circ$, $A_2=0.021\,\mathrm{m}^2$, $A_T=0.1273\,\mathrm{m}^2$, $a_1=2.4176\cdot10^{-5}\,\mathrm{m}^2$, $a_2=2.2421\cdot10^{-5}\,\mathrm{m}^2$, $a_c=6.0465\cdot10^{-6}\,\mathrm{m}^2$. Having modeled all the ASTANK2 components, one can chose either to build up the overall plant model or just some combinations of individual models by connecting them according to a desired process configuration. Subsequently, a range of scenarios could be simulated with the specified configurations.

IV. A SIMULATOR OF ASTANK2

The simulator of the overall ASTANK2 configuration is illustrated in Figure 4. Note that the inputs u, u_1, u_2, u_{11} and u_{22} are the control signals (of continuous variations or ON/OFF type), whereas the outputs h_1, h_2 and h are the measured (observed) signals. Beside the signals in Figure 2, there are three internal signals, namely Q, Q_{pert1} and Q_{pert2}, which indicate the water transport from the lower tank to the upper tanks, through the main and the secondary pipes, respectively. The most complex block in the simulator is the upper tanks module, whose scheme is pointed out in Figure 5.

V. SIMULATON RESULTS

The simulator was tested in different scenarios, by applying step signals of various amplitudes to the simulator inputs. The main interest is to observe the variation of the water levels h_1, h_2 and h. The Figures 6-13 reveal each level variation in response to the input stimuli, by considering a sampling period $T_s=1$ ms. Figure 6-7 present the simulation results for the case when the taps R11, R21 and R are open. Figure 8-9 illustrates the case when R21 is closed. One can see here that h_1 reaches its steady state faster (in 800 s) than h_2 (in 1000 s). Changing the scenario, the behavior in case of supplementary inflows for the upper tanks is simulated. Figures 10 and 11 show the output variations when R11, R21, R are totally open, while R13 and R23 are only 20% open. The first level rises after 200s (the delay of the perturbation signal u_{11}), then it becomes stable. Figures 12 and 13 depict the level variations in case only 70% of perturbations are applied after 100 s and 200 s delay, respectively. One can see that, in all scenarios, the output signals show stabilization, without any controller, even in case of reasonable perturbations, which means that the simulator is an intrinsic stable and robust system.

VI. CONCLUSION

A new multivariable laboratory process (ASTANK2), that consists of two interconnected water tanks with different geometric shapes has been described and analytically modeled. The versatility and modularity of this test-bed allows not only modeling, but also verifying multi-variable system control techniques, which are of great interest in the training process of future professionals.

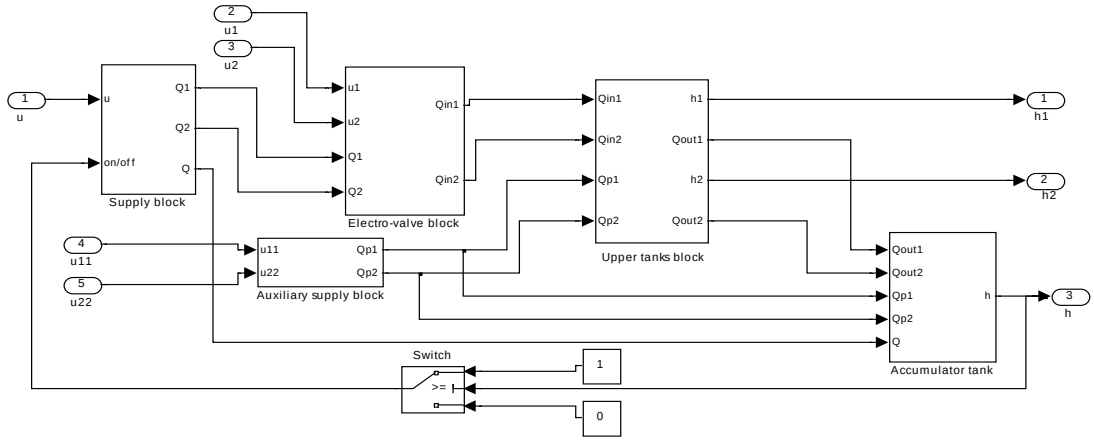

Fig. 4. The Simulink scheme of the overall ASTANK2 model

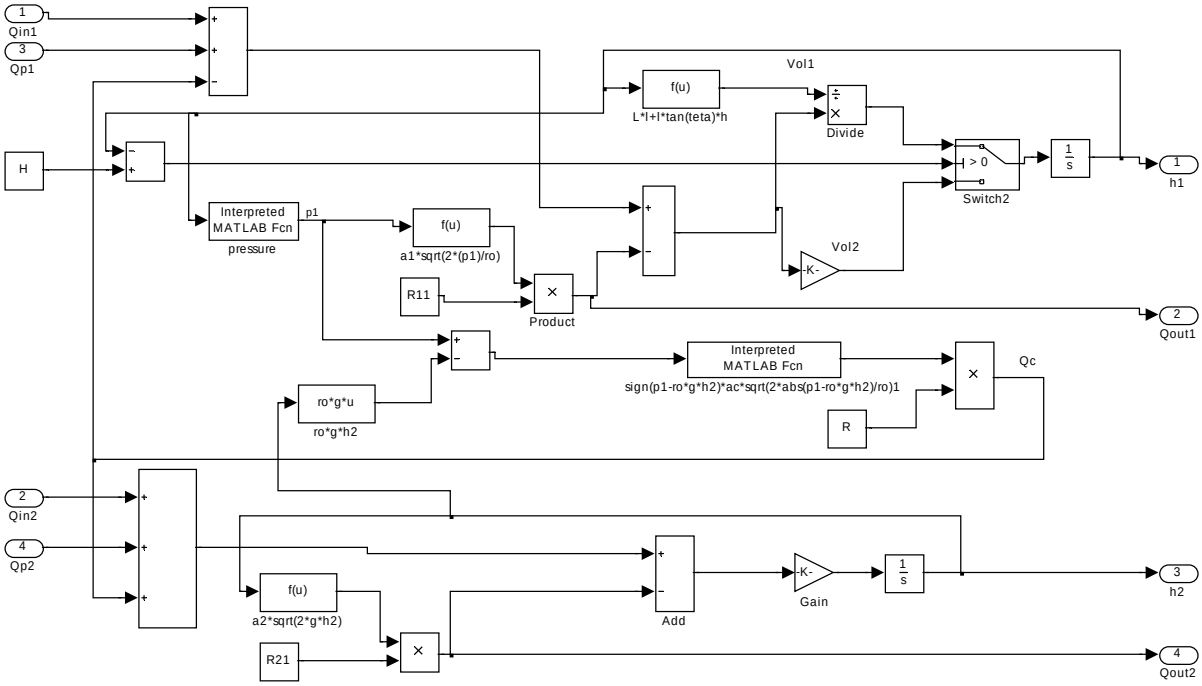

Fig. 5. The upper tank module

VII. References

[1] *** – ASTI Automation SRL: http://www.astiautomation.ro.

[2] *** – INTECO Ltd.: http://www.inteco.com.pl.

[3] Alvaradoa I., Limona D., Muñoz de la Peña D. et al., "A Comparative Analysis of Distributed MPC Techniques Applied to the HD-MPC Four-Tank Benchmark", in Journal of Process Control, Vol. 21, Issue 5, pp. 800–815, June 2011.

[4] Aravind P., Valluvan M., Ranganathan S., "Modelling and Simulation of Non Linear Tank" International Journal of Advanced Research in Electrical, Electronics and Instrumentation Engineering Vol. 2, Issue 2, pp. 842–849, February 2013.

[5] Christy Y., Dinesh Kumar D., "Modeling and Design of Controllers for Interacting Two Tank Hybrid System (ITTHS)", International Journal of Engineering and Innovative Technology (IJEIT), Vol. 3, Issue 7, pp. 88–91, January 2014.

[6] Culita J., Stefanoiu D., "Analytical and Experimental Modeling of Systems", Printech Press, Bucharest, Romania, 2008.

[7] Johansson K.H., "The Quadruple-Tank Process: A Multivariable Laboratory Process with an Adjustable Zero", IEEE Transaction on Control System Technology, vol. 8, no. 3, May 2000.

[8] Nagy A.M., Marx B., Mourot G., Schutz J., "State Estimation of the Three-Tank System Using a Multiple Model", The 48-th IEEE Conference on Decision and Control, China, pp. 7795–7800, December 2009.

[9] Raff T., Huber S., Nagy Z.K., "Allgower, F. Nonlinear Model Predictive Control of a Four Tank System: An Experimental Stability Study", IEEE International Symposium on Intelligent Control, Munich, Germany, pp. 237–242, October 2006.

[10] Shijoh V., Vaidyan M.V., "Development of Nonlinear Model and Performance Evaluation of Model based Controller and Estimator for the Efficient Control of Three-Tank Hybrid System", International Journal of Computer Applications (0975–8887) Volume 56, No.12, October 2012.

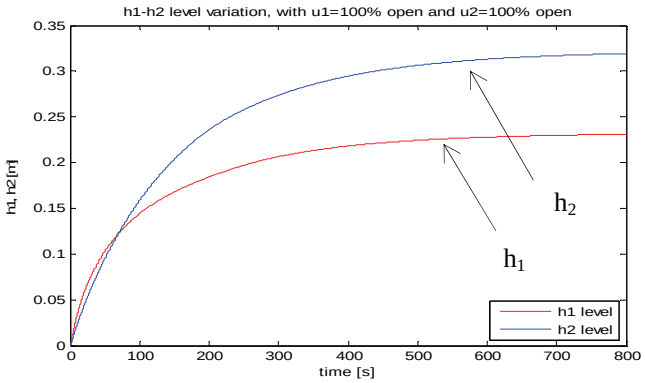

Fig. 6. The h_1, h_2 levels when R11, R21, R are open

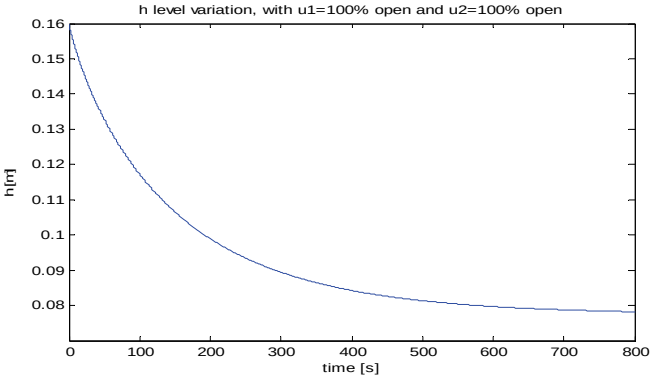

Fig. 7. The h level when R11, R21, R are open

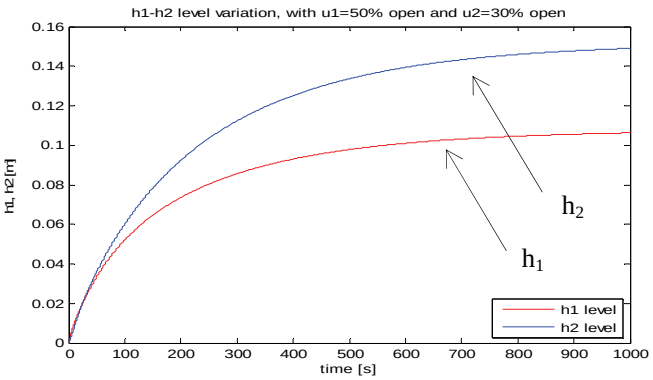

Fig. 8. The h_1, h_2 levels when R11, R are open

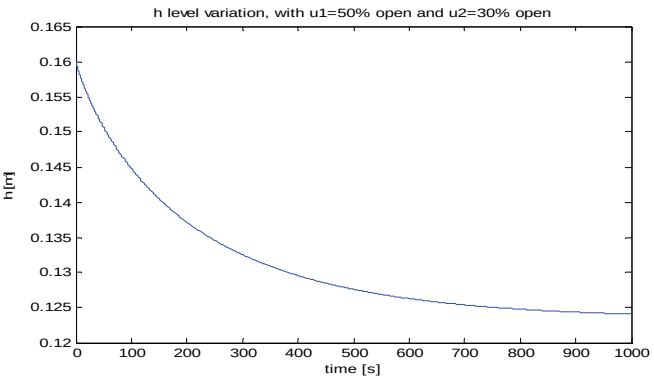

Fig. 9. The h level when R11, R are open

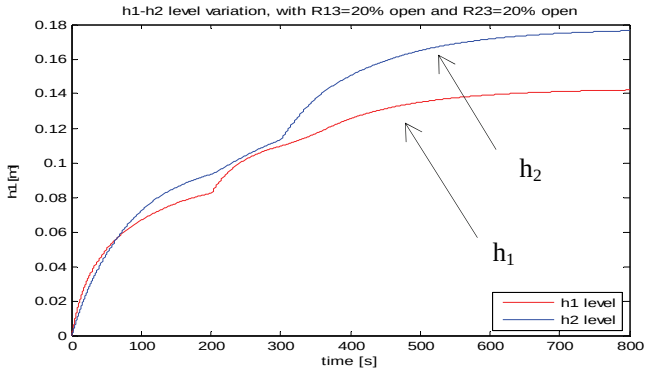

Fig. 10. The h_1, h_2 levels for supplementary inflows (20% of R23, R13)

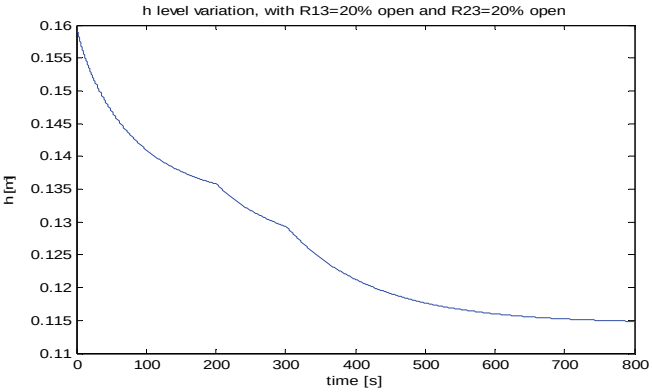

Fig. 11. The h level for supplementary inflows (20% of R23, R13)

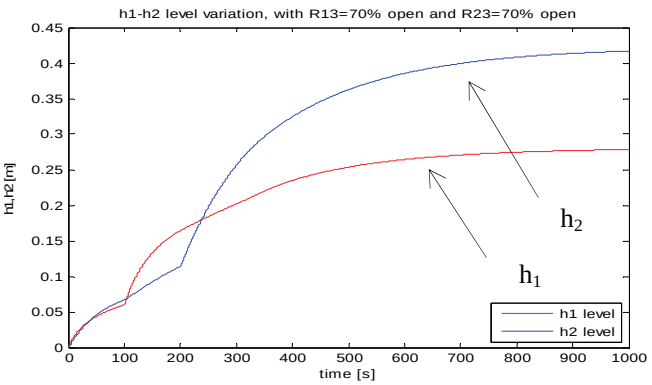

Fig. 12. The h_1, h_2 levels for supplementary inflows (70% of R23 , R13)

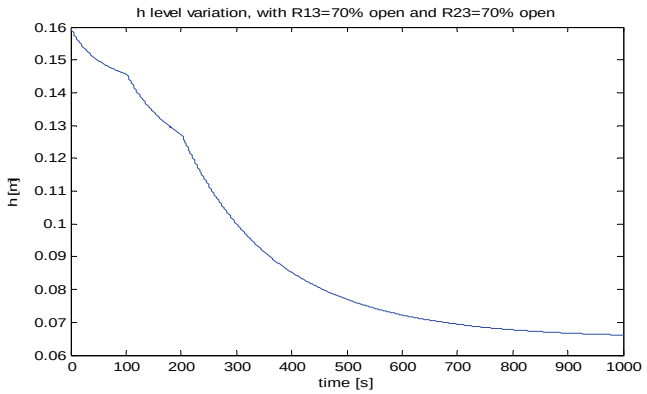

Fig. 13. The h level for supplementary inflows (70% of R23 , R13)